Investigation of MHD Instabilities in an Applied Field MPD Thruster by means of Measurements of Magnetic Field Fluctuations

IEPC-2009-231

Presented at the 31st International Electric Propulsion Conference,
University of Michigan • Ann Arbor, Michigan • USA
September 20 – 24, 2009

M. Zuin[1*], R. Cavazzana[◊], E. Martines[♯]
Consorzio RFX, Padova, Italy

P. Rossetti[§], M. Signori[†], M. Andrenucci[‡], F. Paganucci[♠]
Alta SpA, Pisa, Italy

Abstract: The paper describes the main results of an experimental activity, carried out on a gas fed, applied field MPD thruster. The thruster has operated in a pulsed, quasi-steady mode (pulse length: 5 ms). Magnetic fluctuations in the plasma jet have been measured by means of two non-intrusive sets of magnetic probes. The first set consists of two flux probes, turned around the thruster cylindrical insulator. The probes allow the fluctuations of the magnetic field on the entire length of the thruster to be detected and the axial periodicity in axial direction of the instabilities (mode n) to be obtained. The second set consists of an array of five biaxial probes, placed inside the cylindrical insulator of the thruster. By measuring the magnetic field fluctuations, the array allows the azimuthal periodicity (mode m) to be obtained. Tests have been carried out on the thruster with and without the insertion of an insulating plate in the discharge chamber for passive instability suppression. Magnetic field fluctuations and current-voltage electrical characteristics have been measured for both the thruster configurations at 100 mg/s of argon, external applied magnetic fields B_{ext}= 0, 50, 100 mT on the axis, overall thruster power ranging from 60 and 700 kW. Data gathered have shown the onset of instabilities beyond critical current values, having spatial property of a m/n=1/1 kink, with frequencies close to 400 Hz. The insertion of the plate has proved to effectively reduce fluctuations and arc voltage drop at B_{ext}=100 mT. No significant effects have been observed at lower external magnetic field.

I. Introduction

IN the last years, experimental activities aimed at assessing instability phenomena in MPDTs have been carried out at Alta/Centrospazio in collaboration with Consorzio RFX. Both intrusive (electrostatic and magnetic probes) and non-intrusive (optical probes and ultraviolet tomography) diagnostics have been used[1]. On the basis of measurements

* Researcher, Consorzio RFX, Corso Stati Uniti 4, 35127 Padova, Italy. matteo.zuin@igi.cnr.it

◊ Researcher, Consorzio RFX, Corso Stati Uniti 4, 35127 Padova, Italy. roberto.cavazzana@igi.cnr.it

♯ Researcher, Consorzio RFX, Corso Stati Uniti 4, 35127 Padova, Italy. martines@igi.pd.cnr.it

§ Project Manager, Alta SpA. p.rossetti@alta-space.com

† Former Research Engineer, Alta SpA. Currently: Columbus Operator, ESA/EAC massimiliano.signori@esa.int

‡ Full Professor, Aerospace Engineering Dept., University of Pisa; CEO, Alta SpA, AIAA Senior Member, E.P. Technical Committee, m.andrenucci@alta-space.com

♠ Associate Professor, Aerospace Engineering Dept., University of Pisa; Alta SpA, AIAA Senior Member. f.paganucci@alta-space.com

coming from electrostatic and magnetic probe arrays, the existence of critical regimes has been related to the onset of a basic magneto-hydrodynamic (MHD) instability, well-known in the nuclear-fusion research community as the (m=1; n=1) kink[2]. The limitation of the thrust efficiency has therefore been linked to the Kruskal-Shafranov limit[2,3], as it is well known from experience on fusion devices that the presence of a large MHD instability affects the current profile, and locally modifies the density and temperature of the plasma. Further evidence that the onset of critical regimes in MPDTs is related to the generation of large scale kink modes has been obtained in the framework of an experimental investigation of the thruster plasma plume by means of an integrated system using both electromagnetic and optical probes, and ultraviolet tomography[4].

On the basis of these evidences, different methods of suppressing and/or postponing the onset of the kink instability can be conceived. In previous papers, an attempt of kink instability suppression by inserting in the inter-electrode region insulating plates, extending in a meridian plane, has been illustrated[5,6,7]. The function of the plate is to intercept the helical current components produced by the kink instability, impeding, within a certain extension, the deformation of the plasma column. A variety of geometries of the insulating plate has been tested, measuring overall thruster performance (electrical characteristics and thrust)[6] as well as plasma quantities in the plasma jet by means of electromagnetic probes[7]. As far as concerns the overall thruster performance, previous results indicated the effectiveness of insulating plates for the control of MHD instabilities depends on thruster operation parameters and the geometry of the plate itself. At zero or low applied magnetic field, the plates, independently on the shape and dimension, proved to be ineffective in changing thruster performance, neither improving nor reducing arc voltage drop and thrust at a given current with respect to the thruster without plates. On the contrary, at higher applied magnetic field (50 and 100 mT), some plate configurations proved to reduce considerably the arc voltage drop beyond the critical current, without changing the thrust level. Plasma diagnostic results appeared substantially consistent with the performance results. As matter of fact, the insulating plate placed in front of the cathode region and even small plates located in the outer radial positions are effective in decreasing plasma fluctuations and power losses at higher applied magnetic field. The effect at lower applied field resulted not clear. It has been proven that large plates, extending outside of the inter-electrode region while exhibiting an intense capability of reducing magnetic fluctuations, have a detrimental effect on the power balance of the discharge. Moreover, the diagnostic activity highlighted the importance of measuring plasma fluctuations in the core of the plasma channel in order to correctly relate fluctuations reduction and power balance improvement. Moreover, the influence of spurious effects, like ablation/erosion from electrodes, insulators and plates and vacuum condition remained to be assessed. To this purpose, a new series of tests has been carried out on two thruster configurations (with and without an inter-electrode plate) in an oil free vacuum chamber (IV4), by using two not intrusive sets of magnetic probes, as described in the following paragraphs. The tests herein described were aimed at evaluating the effectiveness of the new diagnostic system to detect and characterize the instabilities as well as at further comparing the thruster operation with and without the inter-electrode plate.

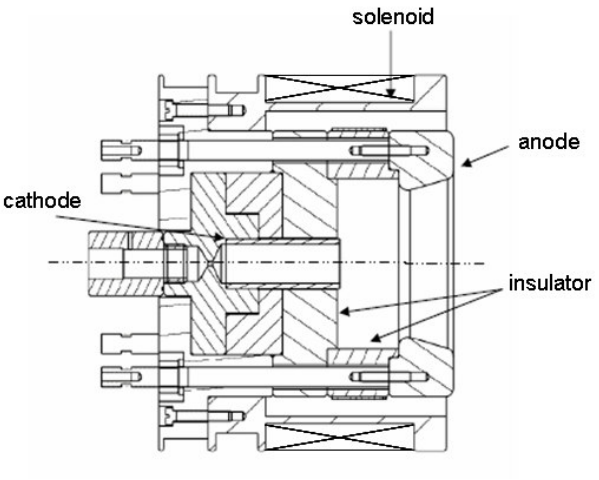

Figure 1: A thruster cross section (benchmark configuration).

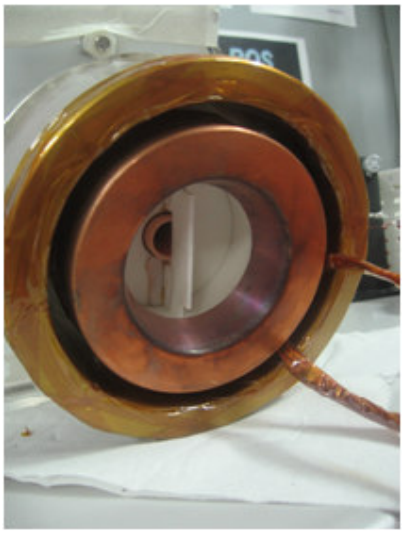

Figure 2: The thruster with the inserted plate (ki-co configuration).

II. Experimental Apparatus

The experimental apparatus consists of an axial-symmetric MPD thruster, with an external solenoid (Fig. 1).It consists of a single channel hollow cathode, 16 mm in inner diameter, and of a ring-shaped anode, 62 mm internal and 108 mm external diameters. The electrodes, made of copper, are separated by an insulator made of MACOR®,

consisting of a back-plate and a cylindrical component, on which the sets of magnetic probes are placed, as illustrated in the following paragraph. The gas propellant is injected throughout the hollow cathode. The coaxial solenoid, equipped with a dedicated power supply described below, allows a magnetic field up to 100 mT on the axis to be applied. The thruster allows plates made of MACOR, 2 mm thick, to be inserted in the inter-electrode region, in a meridian plane, as illustrated in Fig. 2 If necessary, the plates are fixed on the back-plate with a ceramic glue, which can be easily removed after testing. The thruster has been tested in two configurations: without plate (benchmark configuration) and with a plate occupying the total section of the inner plasma channel (kink control (ki-co) configuration, Fig. 2).

III. Diagnostic System

The diagnostic set-up consists of a system of magnetic probes aimed at investigating with high resolution the space and time properties of plasma fluctuations. In particular, the probes used are pick-up probes, i.e. coils turned on an insulating support, producing as output a time varying voltage (V(t)), proportional to the magnetic flux variation, as follows from Faraday's law ($V(t)=-d\Phi(B)/dt$). The geometry and the number of turns used to build the probes have been dimensioned in order to obtain a high frequency response (up to 1 MHz) along with an easily detectable output voltage level.

A 0.2 mm diameter copper wire was used to build the probes, Kapton being the main insulating material with high-vacuum compatibility. Moreover, in order to make the diagnostics non-intrusive for the plasma, the probes have been turned around or inserted in holes drilled in the cylindrical insulator of the thruster, as illustrated in Fig. 3.

The diagnostic system consists of two sets of probes. The first set includes two large coils, which are shown as red rectangles in the scheme of Fig. 3, measuring the flux variation of the axial component of the magnetic field (B_z) on a section of the thruster in the (r,θ) plane in two different axial positions, z = - 32 mm e z = -46 mm, where z=0 is placed at the thruster outlet with positive z pointing outwards.

The second set consists of an azimuthal array of five biaxial magnetic probes, placed inside the cylindrical insulator of the thruster, as shown in Fig. 4. Four probes are equally spaced, measuring the fluctuations of B_r and B_z at r=38 mm and z=-41 mm. To detect azimuthal periodicities till m=4, an additional probe is placed at an intermediate position between two of them. By measuring the magnetic field fluctuations, the array allows the azimuthal periodicity (mode m) to be obtained. For data acquisition a digital oscilloscope was used with a selected sampling rate equal to 5 MHz, in order to ensure a Nyquist frequency larger than the estimated frequency limit of the acquired signals bandwidth.

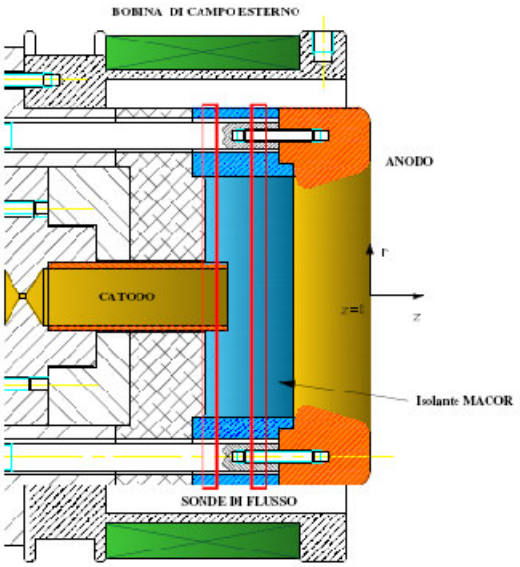

Figure 3: The position of the two sets of magnetic probes. *(red: flux probes; blue: cylindrical insulator, with the five biaxial probes inside)*

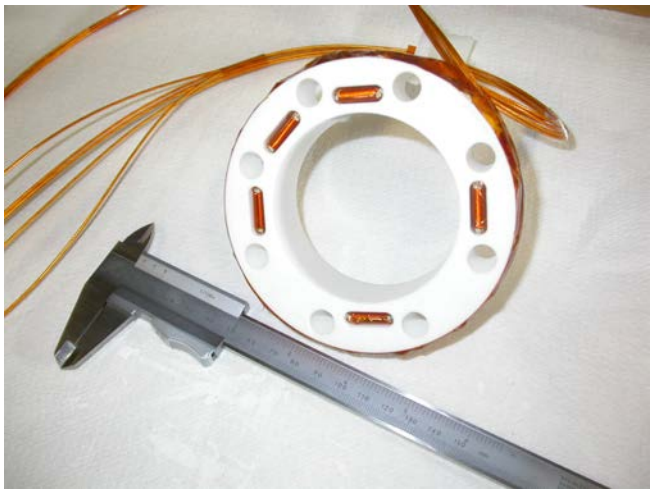

Figure 4: Detail of the cylindrical insulator, with the five biaxial probes.

IV. Test Equipment and Procedure

The thruster has been mounted on a thrust stand inside the service chamber of Alta's IV4 vacuum facility. IV4 consists of a main vessel (Auxiliary Chamber– AC), 2 m in diameter and 2.5 m in length connected through a 1 m gate valve to a service chamber (Small Chamber - SC), 1 m in diameter and 1 m in length. The facility has an overall internal volume of about 9 m^3. The two vessels are both built out of stainless steel AISI 316 L with low magnetic relative

permeability (μ_r<1.06). The main chamber provides the volume for expansion of the beam and contains the main pumping system. The SC is usually dedicated to the installation of the thruster, the thrust stand and all the connections (propellant, power lines, diagnostics) required for the thruster operation. The facility is equipped with two independent completely oil-free pumping systems: one connected to the AC and one connected to the SC for redundancy and emergency operations. The main pumping system includes a 25 m^3/hr rotary pump, a 2000 l/s turbo-molecular pump and a cryogenic high vacuum stage (not used for the tests herein described). The chamber has been evacuated till a pressure in the range of 10^{-5} mbar before each shot. The back pressure did not exceeded $2x10^{-4}$ mbar during each shot.

The electric power is supplied by a Pulse Forming Network (PFN), configured to supply quasi-steady current pulses 5 ms long. The propellant is injected through the hollow cathode by means of a fast acting solenoid valve, which provides gas pulses with long plateau after few milliseconds from valve activation. The external magnetic coil of the thruster is supplied by the discharge of a 10 mF capacitor bank by means of an SCR. As shown experimentally, a quasi-steady magnetic field lasting about 10 ms is obtained after 20 ms from the SCR switching on[8]. An ignitron has been used to initiate the discharge when steady applied magnetic field and mass flow rate are reached. Each shot has been performed by charging the PFN at a given voltage. A laboratory-made digital device allows to set the sequence of the SCR, the solenoid valve activation and the ignitron switching on, in order to start the arc discharge when a steady condition is reached for both the applied magnetic field and the mass flow rate.

The arc current has been measured with a Hall effect current probe. To avoid anomalous discharge involving the vacuum chamber, the thruster electrodes are floating with respect to the ground and the arc voltage has been measured by measuring the potential of each electrode with respect to the ground by means of two high voltage probes. The arc voltage is then obtained by subtracting the cathode voltage signal from the anode voltage signal.

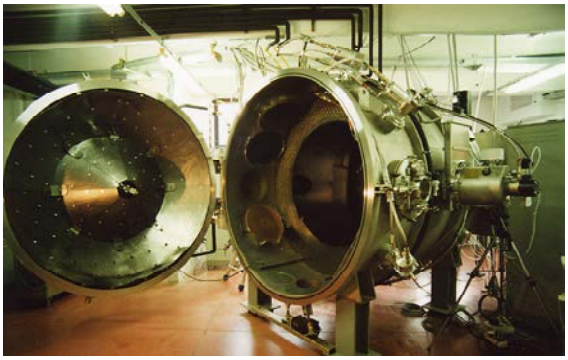

Figure 5: Alta's IV4 vacuum facility.

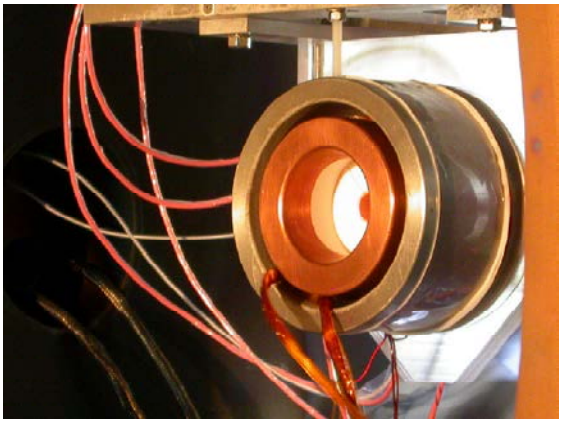

Figure 6: the thruster mounted on the thrust stand in the vacuum facility.

V. Data Analysis Technique

In the following paragraph, the characterization of kink modes has been performed by means of the reconstruction of the spectral density, starting from the measured probe signals. The two-point technique is used to reconstruct the spectral density S(k,f), where k is the wave number in the direction along which the two probes are aligned and f is the frequency. The technique is performed on a statistical basis and proceeds as follows: the signals y_1 and y_2 coming from two probes are divided into N slices of equal length, $y1^{(i)}$ and $y2^{(i)}$ (i=1,…,N). The slices are considered as independent realizations of the stochastic process under study. For each slice, the discrete Fourier transforms $\psi_1^{(i)}(f)$ and $\psi_2^{(i)}(f)$ are obtained. From these, the power $S^{(i)}(f)=(|\psi_1^{(i)}(f)|^2 + |\psi_2^{(i)}(f)|^2)/2$ and the cross-phase $\alpha^{(i)}= \arg\{([\psi_1^{(i)}(f)]^* \psi_2^{(i)}(f)\}$ are calculated. The cross-phase is used to obtain an estimate of the wave number in the direction connecting the two probes, $k^{(i)}(f)=\alpha^{(i)}(f)/\Delta x$, where Δx is the distance between the probes. These results are used to progressively fill a histogram of the spectral density, i.e., for each frequency f the bin corresponding to the wave number $k^{(i)}(f)$ is increased by the amount $S^{(i)}(f)$.

By repeating this procedure for all of the slices, the resulting histogram of S(k, f) is a statistical estimate of the true spectral density function. In this procedure, several assumptions are hidden: the process under study is assumed steady (at least with respect to the fluctuation time scale) and Δx is much smaller than the fluctuation wavelength.

VI. Experimental Results

Tests described below have been carried out by using argon as propellant, at 100 mg/s of mass flow rate during the steady phase of the pulse. Magnetic field fluctuations from the two sets of probes and current-voltage electrical characteristics have been measured for external applied magnetic fields B_{ext}= 0, 50, 100 mT (maximum value on the axis). PFN charging voltage has been spanned to get both sub and supercritical discharge currents at the various applied magnetic fields, as shown in Tab. 1[2,9]. Overall power thruster has ranged between 60 and 700 kW.

Applied Magnetic Field (mT)	Critical Current (kA)
0	2.3
50	2.1
100	1.5

Table 1 Calculated critical currents for the MPD thruster investigated. *Benchmark configuration at 100 mg/s of argon, in accordance with Ref. 2 and 9.*

Instability Assessment

The first series of tests has been carried out on the benchmark configuration and was aimed at assessing plasma instabilities. In Fig. 7 the typical time traces of discharge current (I_p) and arc voltage (ΔV) signals are shown for both a sub-critical and a super-critical condition, with B_{ext}=100 mT. The growth of large fluctuations on both I_p and ΔV signals is evident when the threshold plasma current is exceed.

The generation of large fluctuations is even clearer on the magnetic (dB/dt) signals coming from the biaxial and the flux probes, shown on the right hand side of the same figure, for the same experimental conditions.

An analysis of the time spectral components of these fluctuations is reported in Fig. 8 in the form of a colour coded spectrogram contour plot showing the time behaviour of the power spectrum of a signal from a single flux probe. The spectrograms are evaluated for three different plasma current levels, in discharges with B_{ext}=100 mT, whose time traces are shown in the top part of the figure.

The transition from sub-critical to critical condition is associated to the generation of increased magnetic fluctuations which appear to have a coherent behaviour, in the form of a mode with a well defined frequency above 300 kHz. At the highest plasma current the mode exhibits a broader frequency spectrum, centred around 400 kHz.

The azimuthal array of probes has been used to Fourier deconvolve in space the observed magnetic fluctuations. In particular, Fig. 9 shows the time behaviour of amplitude of the m=0 and m=1 azimuthal mode number for a discharge with I_p=3000 A. The m=1 is found to be the dominant azimuthal periodicity, although a non negligible m=0 component is also present, with a good time-correlation with the m=1 component. A more detailed assessment of the mode m has been performed by applying the two-point technique described before to the signals gathered by the fifth azimuthal probe (45° shifted), for the time interval indicated by the dashed lines in Fig. 9.

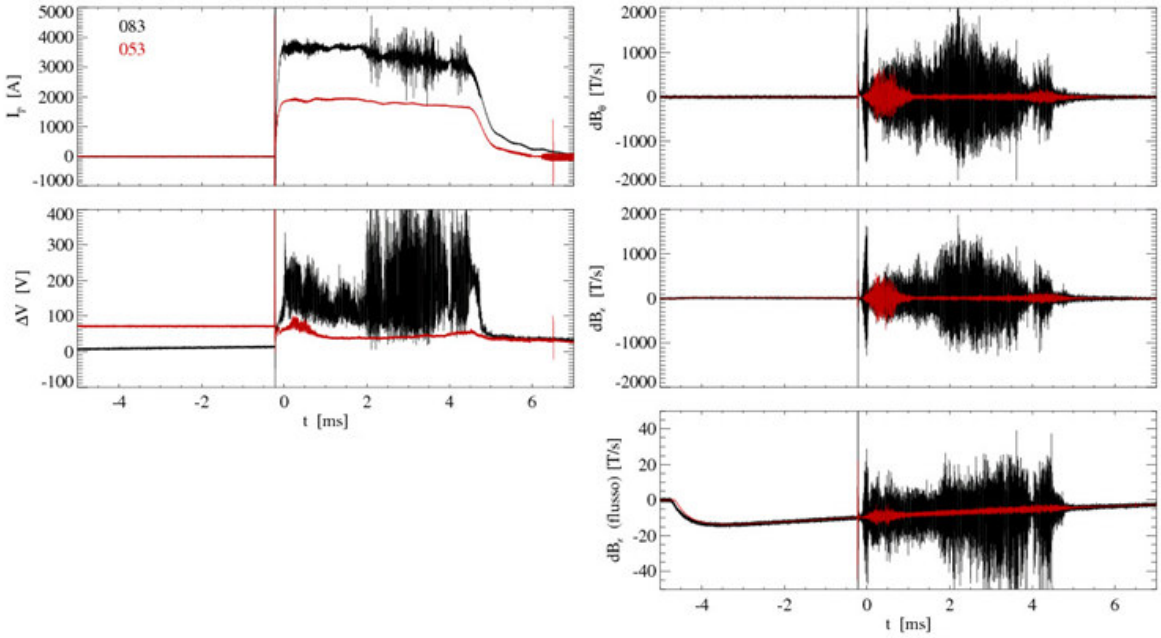

Figure 7: Comparison between sub-critical (red) and super-critical (black) thruster operation. *Benchmark configuration, B_{ext}=100 mT; on the left from the top: total arc current and voltage signals; on the right from the top: azimuthal and axial magnetic field fluctuations from a biaxial probe of the azimuthal array, axial magnetic field fluctuation from a flux probe.*

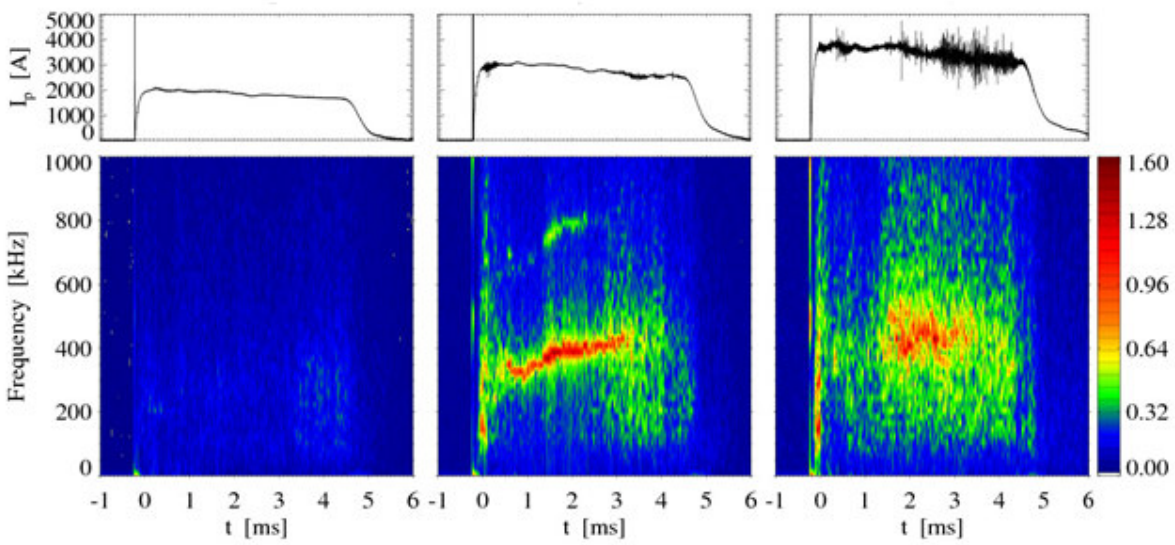

Figure 8: Spectrograms of the signal coming from a flux probe at three arc current levels. *Benchmark configuration, B_{ext}=100 mT.*

The relevant space-time analysis, shown in Fig. 10 in a colour coded contour plot, exhibits a clear peak corresponding to m=1 azimuthal mode number and to a frequency around 300 kHz, the same as that already observed in the spectrogram of a single probe signal (higher order harmonics in both frequency and mode number can also be observed).

By means of the two flux probes at two different axial positions, and applying again the two-point techniques, it is possible to perform an analysis of the space-time properties of the magnetic fluctuations along the axial direction, in particular it is possible to deduce the axial wave-vector, k_z. It must be said that as the probes measure fluctuations of the magnetic flux on the total plasma section, only the m=0 component can be analysed in this way, but due to the strong time-correlation between m=0 and m=1 mode amplitude, shown in Fig. 9, it is reasonable to believe that the information about the axial periodicities obtained in this way, can be extended to the global magnetic fluctuations.

As shown in Fig. 11, the fluctuations at ≈400 kHz are associated to a peak in the $S(k_z,f)$ spectra, corresponding to an axial wavelength $\lambda_z(=2\pi/k_z)$ of the order of 10 cm, thus comparable to the thruster size.

This observation suggests that the magnetic activity is produced by a fast rotating m=1 structure, with the features of a kink instability, thus confirming the results previously obtained on MPD thrusters with different size and geometry[1,2,3,4].

It is interesting to note that the frequency here detected is noticeably higher than those measured in previous studies, which suggests an important role of the dimension of the plasma column and, in particular, of the thruster size on the velocity of the rotation of the kink instability. This result could be interpreted in terms of a dependence of the frequency of the kink rotation on the plasma flow (and in the MPD case on acceleration produced by the Lorentz force) as recently demonstrated by Furno et al. [10].

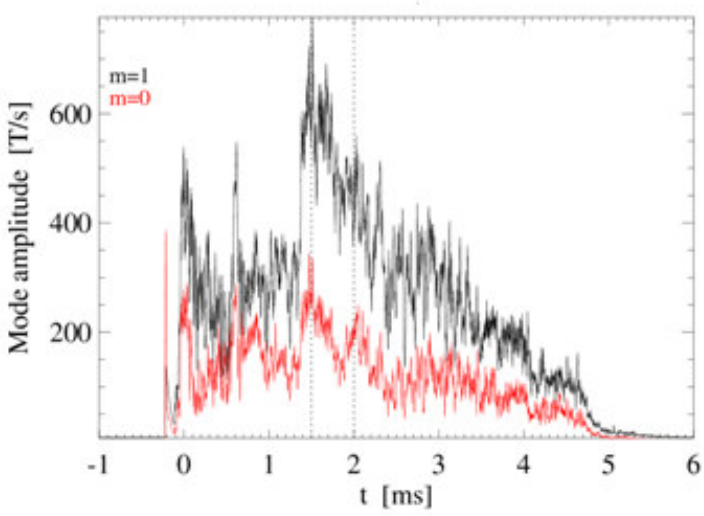

Figure 9: Mode m amplitude during a shot. *Benchmark configuration, B_{ext}=100 mT, I_p≈3000 A.*

The analysis of the spectral properties of the magnetic fluctuations for a self-field operation (B_{ext}=0mT) reveals that a mode rotating at a frequency centred around 200 kHz (with a rather broad spectrum) forms only at the highest plasma current levels explored (Fig. 12), giving rise to a magnetic fluctuation amplitude much lower than that observed at B_{ext}=100mT (note the different colour scale of Fig. 12 with respect to Fig. 8). This occurrence could indicate the thruster was probably working in a marginally critical condition when operated in the self-field configuration.

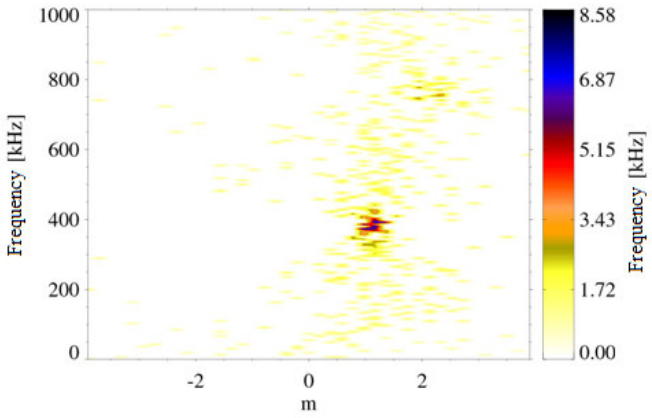

Figure 10: Mode m (azimuthal) characterization (two-point technique used). *Benchmark configuration, B_{ext}=100 mT, I_p≈3000 A.*

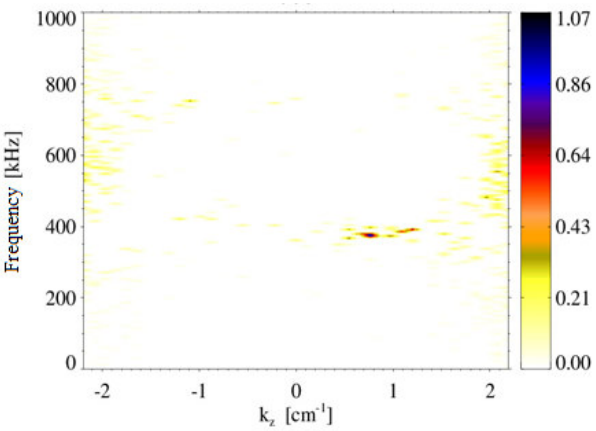

Figure 11: Mode n (axial) characterization (two-point technique used). *Benchmark configuration, B_{ext}=100 mT, I_p≈3000 A.*

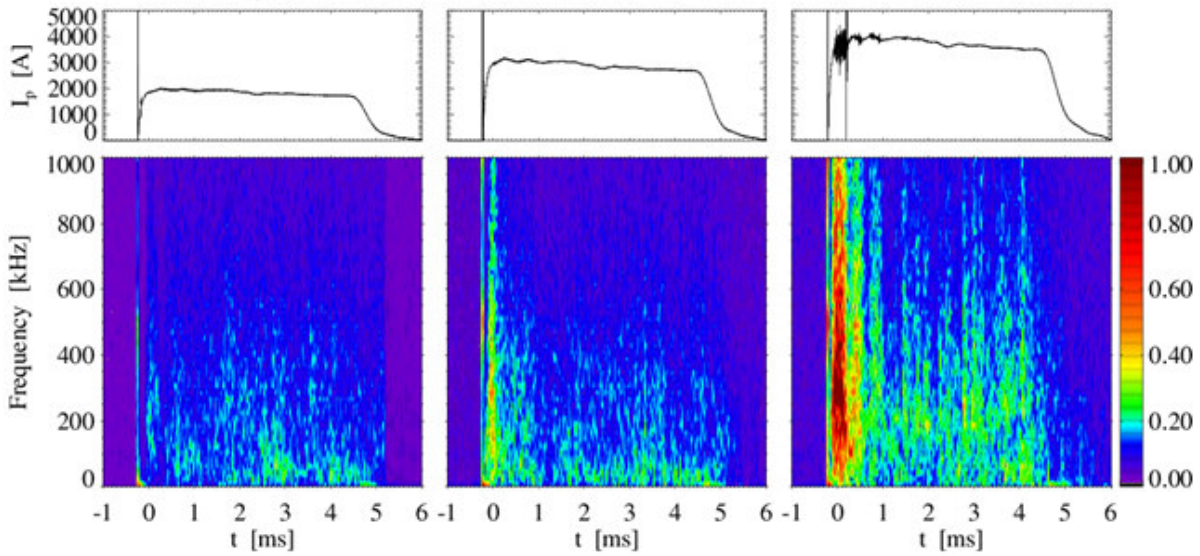

Figure 12: Spectrograms of the signal coming from a flux probe at three arc current levels. *Benchmark configuration, B_{ext}=0 mT.*

Benchmark and Ki-co Configuration Comparison

The second series of tests was aimed at comparing the two configurations in terms of electrical characteristics and total magnetic fluctuation levels (by integrating the power spectra over all frequencies), measured by the two sets of magnetic probes. Each data point in the following figures represents average values of the relevant quantities, measured for four-five shots at the same PFN charging voltage. For each shot, a value of arc voltage, current and magnetic fluctuation from the various probes were obtained as an average on a window 100 microseconds long taken in the middle of the pulse. Error bars include both standard deviation and measurement uncertainty. An example of signals measured on the two configurations at the same current and applied magnetic field (100 mT) is shown in Fig. 13. In this particular case, the reduction of the magnetic fluctuation levels in super-critical condition observed in ki-co configuration is accompanied by a reduction of the fluctuation of both plasma current and applied voltage signals. In this case, the ki-co actually seems to drive the super-critically operating thruster to a sub-critical operation.

A comparison in terms of electrical characteristics between benchmark and ki-co configurations is shown in Fig. 14. At low current levels, ki-co seems to have no significant effects on arc voltage for all the applied magnetic fields investigated. At 100 mT, ki-co tends to reduce arc voltage, data dispersion and fluctuation at currents higher than about 2 kA. In particular, a decrease of a 30% of the applied voltage at the highest plasma current has been measured.

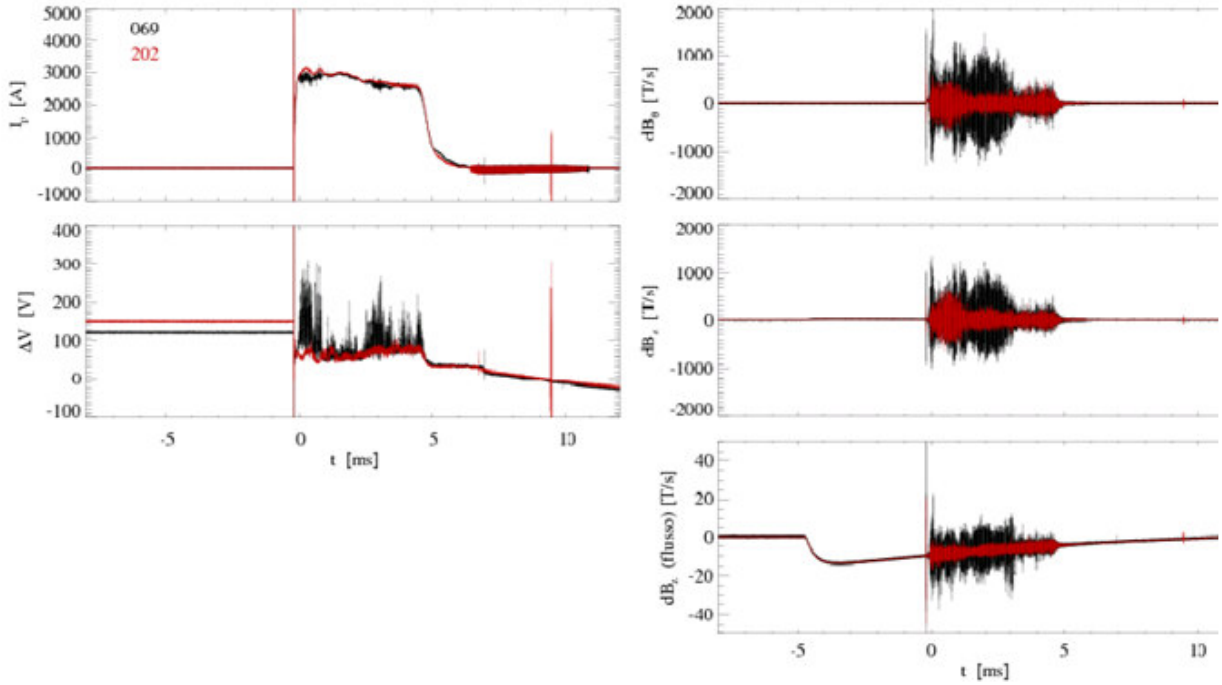

Figure 13: Comparison between signals gathered on benchmark (black) and ki-co (red) configurations. *B_{ext}=100 mT; on the left from the top: total arc current and voltage signals; on the right from the top: azimuthal and axial magnetic field fluctuations from a biaxial probe of the azimuthal array, axial magnetic field fluctuation from a flux probe.*

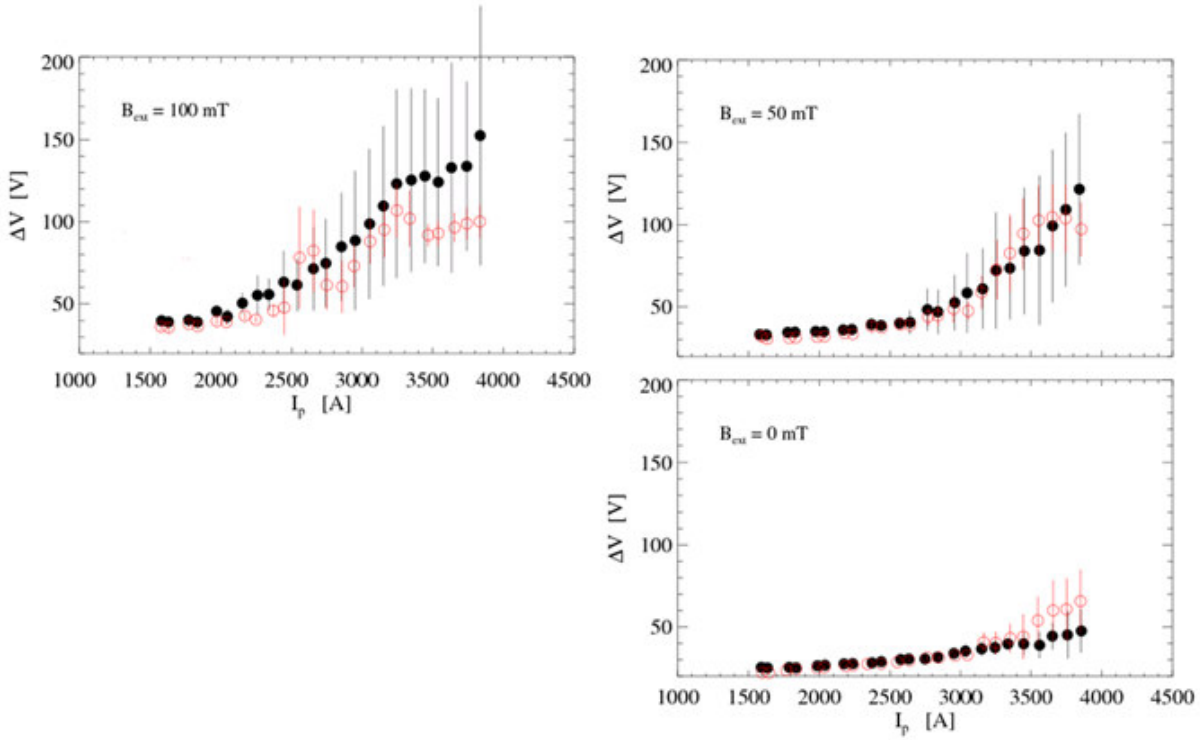

Figure 14: Electrical characteristic comparison at different B_{ext} between benchmark (black spots) and ki-co (red circles) configurations.

At 50 mT, no significant variations of arc voltage have been observed also at supercritical currents, although both data dispersion and fluctuation are reduced with respect to benchmark operation. At 0 mT, ki-co seems to have a detrimental effect on electrical characteristics, increasing arc voltage , data dispersion and fluctuation at currents higher than 3.4 kA. The plot referring to the B_{ext}=100mT (and also B_{ext}=50mT) case shows a clear drop of the magnetic fluctuation level measured by the flux probes in the two axial positions, with the increase of the plasma current above 2.5 kA, the plot referring to the B_{ext}=0mT does not highlight any clear indication of a super-critical condition.

The comparison of benchmark and ki-co configurations in terms of total magnetic fluctuations, obtained by signals measured by the two sets of magnetic probes, is shown in Figs 15 and 16. Graphs in Fig. 15 indicate a significant reduction of the amplitude of the magnetic perturbation, increasing with the increase of the plasma current, has been observed with ki-co with respect to benchmark at 100 mT. A clear modification of the magnetic fluctuation level has been observed at 50 mT only for currents higher than 3.5 kA. The reduction of the magnetic fluctuation is visible in both the axial positions explored (Fig. 16), indicating that a real reduction of the amplitude of the global kink mode was produced by the ki-co. For self-field operation (0 mT), a slight detrimental effect is observed in the ki-co with respect to the benchmark configuration.

It is interesting to note that at 0mT, ki-co does not seem to affect the magnetic perturbation at low plasma current, while it induces an increase of the fluctuation level for current exceeding 3 kA. The ki-co, in this case, having a detrimental effect on the plasma, drives an almost quite plasma to a super-critical condition, favouring the generation of a large scale mode. The reason for this behaviour is still totally unclear.

The analysis of the fluctuation levels measured by the two axial probes in Fig. 16 shows that the beneficial effect of the ki-co on the plasma is confirmed for the cases 50 and 100 mT, while an increase of the rms of the signals, produced by the ki-co, can be seen for self-field operation.

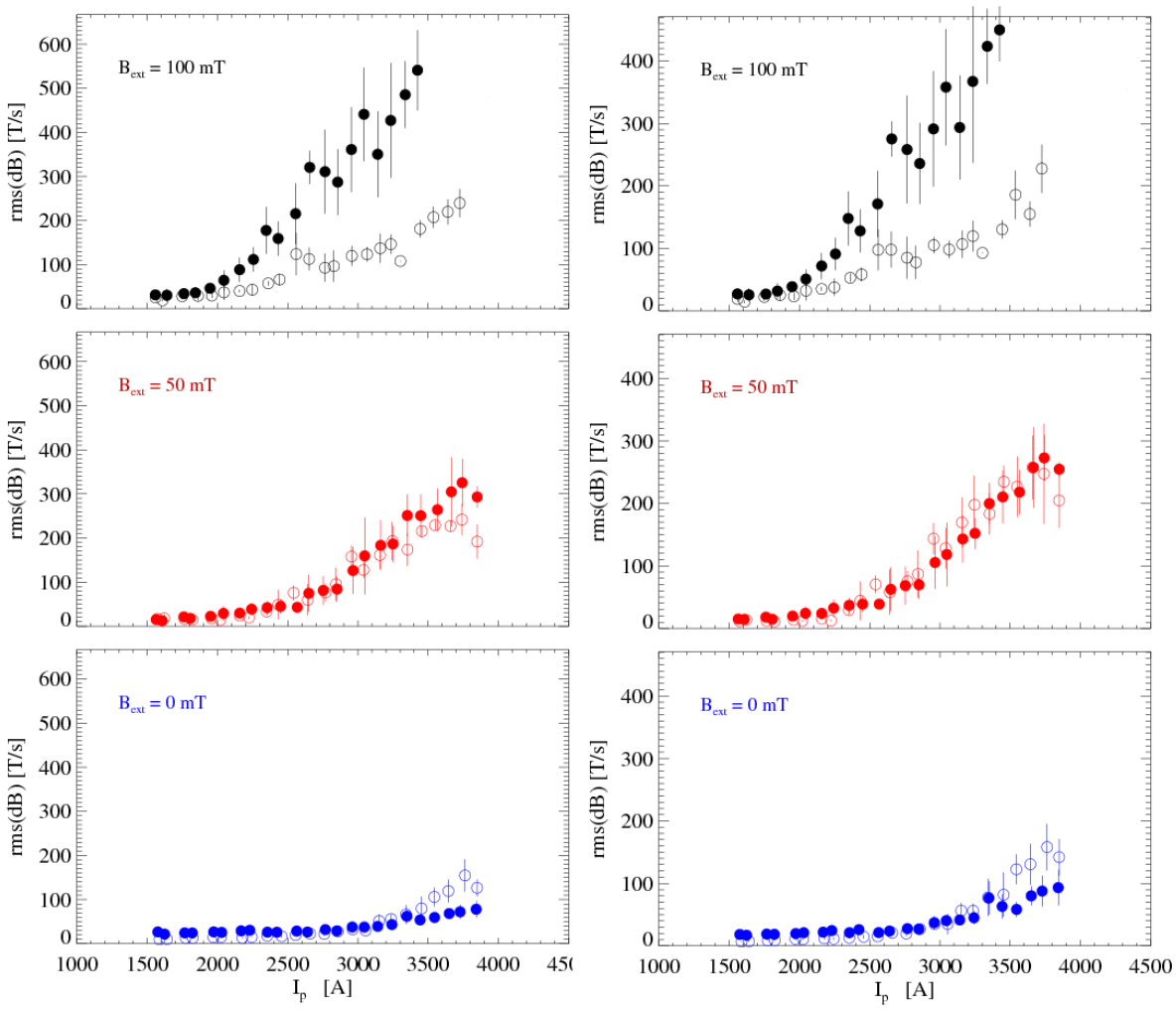

Figure 15: rms values vs arc current of signals measured by a biaxial probe at different B_{ext}, for benchmark (spots) and ki-co (circle) configurations. *On the left: azimuthal component (B_θ); on the right: axial component (B_z).*

VII. Conclusion

The experimental results illustrated in this paper have demonstrated the not intrusive diagnostic system developed, based on two sets of magnetic probes, is effective in detecting and characterizing gross MHD instabilities occurring in MPD thrusters. Results obtained are in substantial agreement with what observed in previous tests on the same and other MPD thrusters, carried out at Alta/Centrospazio. The frequencies here detected are noticeably higher than those measured in previous experiments, which suggests an important role of the dimension of the plasma column and, in particular, of the thruster size on the velocity of the rotation of the kink instability.

Results obtained by magnetic fluctuation measurements are consistent with electrical characteristic measurements, both for benchmark and ki-co configuration. As a matter of fact, a strong correlation between plasma fluctuation level and power level can be clearly inferred for all the conditions investigated.

Tests have shown the effect on the performance of the inter-electrode plate strongly depends on the applied magnetic field and current levels. In particular, plate insertion seems to effectively interact with the instability at higher applied magnetic field (higher than 50 mT), with no significant or detrimental effects at a self-field operation.

Since no thrust measurements have been performed during tests, it is not possible to rigorously compare the operation of the two thruster configurations in terms of specific impulse and thrust efficiency. To this regards, tests herein illustrated must be considered preliminary to a further experimental activity which will be carried out in the future.

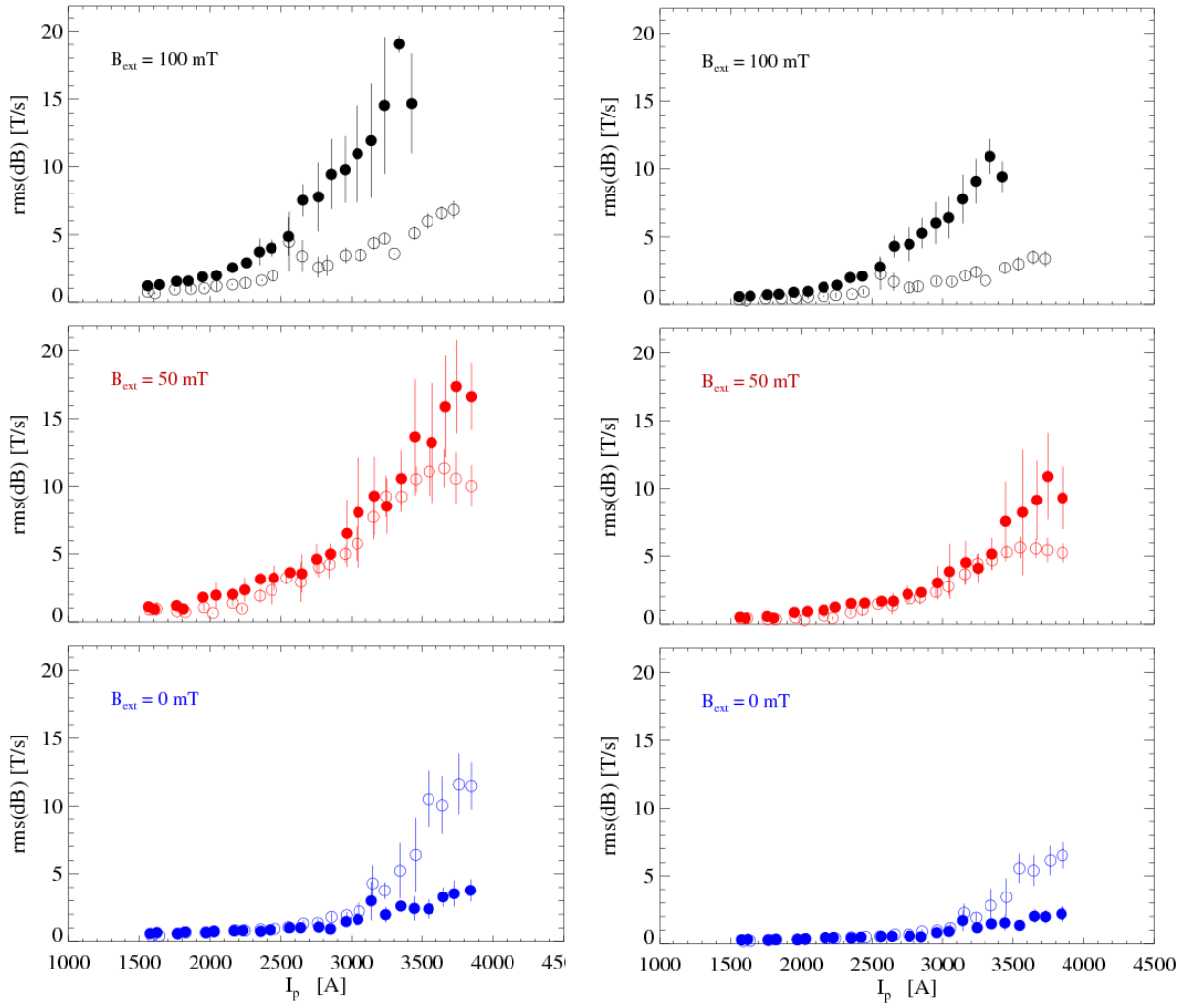

Figure 16: rms values vs arc current of signals measured by the flux probes (B_z) at different B_{ext}, for benchmark (spots) and ki-co (circle) configurations. *On the left:: probe at z=-46 mm; on the right: probe at z=-32 mm.*

References

[1] F. Paganucci, M. Zuin, M. Agostini, M. Andrenucci, V. Antoni, M. Bagatin, F. Bonomo, R. Cavazzana, P. Franz, L. Marrelli, P. Martin, E. Martines, P. Rossetti, G. Serianni, P. Scarin, M. Signori and G. Spizzo, "*MHD Instabilities in Magneto-Plasma-Dynamic Thrusters"*, Plasma Phys. Control Fusion **50** 124010 (2008).

[2] M. Zuin, R. Cavazzana, E. Martines, G. Serianni, V. Antoni, M. Bagatin, M. Andrenucci, F. Paganucci, P. Rossetti, "*Kink instability in applied field MPD thruster"*, Phys. Rev. Lett. **92**, 225003 (2004).

[3] M. Zuin, R. Cavazzana, E. Martines, G. Serianni, V. Antoni, M. Bagatin, M. Andrenucci, F. Paganucci, P. Rossetti, *Critical Regimes and MHD Instabilities in a Magneto-Plasma-Dynamic Thruster*, Phys. Plasmas **11**(10), 4761 (2004).

[4] F. Bonomo, P. Franz, G. Spizzo, and L. Marrelli, P. Martin, F. Paganucci, P. Rossetti, M. Signori, M. Andrenucci, N. Pomaro, *"Ultraviolet tomography of kink dynamics in a magnetoplasmadynamic thruster"*, Phys. Plasmas **12**(09), 3301 (2005).

[5] E. Martines, F. Paganucci, M. Zuin, M. Bagatin, R. Cavazzana, P. Rossetti, G. Serianni, M. Signori, V. Antoni, M. Andrenucci, "*Performance Improvement due to Kink Instability Suppression in MPD Thruster*", IEPC-2005-231, 29th International Electric Propulsion Conference, Princeton (NJ), Oct. 31 – Nov. 4, 2005.

[6] F. Paganucci, P. Rossetti, M. Andrenucci, M. Zuin, V. Antoni, R. Cavazzana, M. De Tata, E. Martines, G. Serianni, and F. Tarallo, *"Experimental Assessment of a Passive Method for MHD Instability Suppression in MPD Thrusters*", IEPC-2007-330, 30th International Electric Propulsion Conference, Florence, Italy, September 17-20, 2007.

[7] M. Zuin, M. Andrenucci, V. Antoni, R. Cavazzana, M. De Tata, E. Martines, F. Paganucci, P. Rossetti, G. Serianni, F. Tarallo, "*Magnetic Fluctuations in a MPD Thruster with Passive Systems for the Control of MHD Instabilities*", IEPC-2007-331, 30th International Electric Propulsion Conference, Florence (I), Sept. 17-20, 2007.

[8] U. Cesari, *"Studio e caratterizzazione del campo magnetico applicato in un propulsore MPD"*, Laurea Thesis, A-A 1999-2000, University of Pisa.

[9] F. Paganucci, P. Rossetti, M. Andrenucci, V.B. Tikhonov, V.A. Obukhov, *"Performance of an Applied Field MPD Thruster"*, IEPC-01-132, 27th International Electric Propulsion Conference, Pasadena, CA, October 14-19, 2001.

[10] I. Furno et *al.*, Phys. Rev. Lett. 97, 015002 (2006)